



LETTER • OPEN ACCESS

The spatial-temporal distributions of controlling factors on vegetation growth in Tibet Autonomous Region, Southwestern China

To cite this article: Guangyong You *et al* 2019 *Environ. Res. Commun.* 1 091003

View the [article online](#) for updates and enhancements.

You may also like

- [Regional adaptation of a dynamic global vegetation model using a remote sensing data derived land cover map of Russia](#)
S Khvostikov, S Venevsky and S Bartalev
- [Potential pollen evidence for the 1933 M 7.5 Duxi earthquake and implications for post-seismic landscape recovery](#)
Hongyan Xu, Hanchao Jiang, Kam-biu Liu et al.
- [Inter-annual Climate Variability and Vegetation Dynamic in the Upper Amur \(Heilongjiang\) River Basin in Northeast Asia](#)
Guangyong You, M Altaf Arain, Shusen Wang et al.

Environmental Research Communications



LETTER

The spatial-temporal distributions of controlling factors on vegetation growth in Tibet Autonomous Region, Southwestern China

OPEN ACCESS

RECEIVED
10 July 2019REVISED
18 August 2019ACCEPTED FOR PUBLICATION
21 August 2019PUBLISHED
5 September 2019

Original content from this work may be used under the terms of the [Creative Commons Attribution 3.0 licence](#).

Any further distribution of this work must maintain attribution to the author(s) and the title of the work, journal citation and DOI.



Guangyong You¹ , M Altaf Arain², Shusen Wang³, Shawn McKenzie², Changxin Zou¹, Zhi Wang¹, Haidong Li¹, Bo Liu⁴, Xiaohua Zhang⁵, Yangyang Gu¹ and Jixi Gao^{1,6}

¹ Nanjing Institute of Environmental Sciences, Ministry of Ecology and Environment, Nanjing, Jiangsu, 210042, People's Republic of China

² School of Geography and Earth Sciences and McMaster Centre for Climate Change, McMaster University, Hamilton, Ontario L8S 4K1, Canada

³ Canada Centre for Remote Sensing, Natural Resources Canada, Ottawa, Ontario K1A0E4, Canada

⁴ School of Remote Sensing and Geomatics Engineering, Nanjing University of Information Science and Technology, Nanjing, Jiangsu, 210044, People's Republic of China

⁵ School of Applied Meteorology, Nanjing University of Information Science and Technology, Nanjing, Jiangsu, 210044, People's Republic of China

⁶ Author to whom any correspondence should be addressed.

E-mail: gjx@nies.org

Keywords: climate change, vegetation activity, change point detection, controlling factors

Abstract

Due to cold and arid climate of Tibet Autonomous Region, vegetation growth is considered to be controlled by both moisture availability and warmth. In order to reveal the patterns of regional climate change and the mechanisms of climate-vegetation interactions, long term (1982–2013) datasets of climate variables and vegetation activities were collected from Climatic Research Unit (CRU) and Global Inventory Monitoring and Modeling System (GIMMS). Principal regression analysis and (partial) correlation analysis were conducted to reveal the contributions of controlling factors on vegetation growth. Study results showed that (1) Annual mean air temperature (TMP) had increased by 0.38 °C per decade ($P = 0.00$) and annual precipitation (PRE) had increased by 17.25 mm per decade ($P = 0.15$). A significant change point around the year 1997/1998 was detected by Mann-Whitney-Pettit test, coinciding with the occurrence of El Niño event. (2) Normalized Difference Vegetation Index (NDVI) had an insignificant positive trend. Spatially, pixels of high NDVI values, great NDVI trends and high inter-annual deviations are distributed in the densely vegetated eastern part. Principal regression analysis revealed that, alpine grassland (northern and western part) is mostly controlled by temperature, steppe meadow (middle and southern part) is mostly controlled by precipitation, and shrub/mixed needle leaved and broad leaved forest (eastern part) is mostly controlled by cloud coverage. (3) Partial correlation analyses showed that regions with high sensitivity to precipitation nearly overlapped with regions of high sensitivity to minimum temperature. And the high importance of cold index (CDI, accumulated negative difference between TMP and 5 °C) revealed in this study implied the effects of regional glacial melting and permafrost degradation. We concluded that the regional climate change can be characterized as warming and wetting. Different regions and vegetation types in Tibet Autonomous Region demonstrated different driving climate factors and climate-vegetation relationships.

1. Introduction

The Tibetan Plateau is located in southwestern China and considered as the 'Third Pole' of the Earth. It provides various ecosystem services for human beings, including climate regulation, water resources retention, biodiversity conservation and regional/national eco-security protection. With high sensitivity to climate

warming and an average altitude exceeding 4000 m a.s.l., TP is also a hot spot for studies of climate-vegetation interactions (Kim *et al* 2012, Huang *et al* 2016, Cong *et al* 2017).

In recent years, a growing number of studies on the regional climate-vegetation relationship provided controversial results. For example, studies revealed that water availability is considered as the main limiting factor for plant growth (Yang *et al* 2010, Kulkarni 2012, Zeppel *et al* 2014) and phenological changes (Shen *et al* 2015, Wang *et al* 2015) over the Tibetan Plateau. Whereas, other studies highlighted temperature as an important constraint due to the cold environments (Zhang *et al* 2014, Shi *et al* 2019). In addition, more studies have recognized the role of asymmetric warming, which is characterized as higher trend of diurnal minimum temperature than maximum (You *et al* 2016), played in controlling the plant phenology and vegetation dynamics (Yang *et al* 2017).

Besides the controversial conclusions on controlling factors for vegetation activity, the spatial pattern of vegetation growth responding to climate change remains unclear. Different vegetation types (Zhu *et al* 2017) and regions (Wang *et al* 2015) have different pattern of climate-vegetation interactions, resulting in a considerable spatial heterogeneity of vegetation activity (Huang *et al* 2016).

Therefore, sensitivity analyses of vegetation dynamics to climatic variables are essential to understanding the relationship between the regional climate change and vegetation dynamics. Moreover, understanding the ecological effects of climate change on the Tibetan Plateau is of great significance to improve environmental management and to promote regional sustainable development (Guo *et al* 2014).

With datasets collection of climate variables and vegetation activities in the Tibet Autonomous Region, this study tries to address the following questions: (1) what are the temporal patterns of changes in climate factors and vegetation activity in this region? (2) what are the ecological effects of climate change (especially asymmetric warming) on vegetation dynamics? (3) what is the spatial distribution of the vegetation sensitivity to different climate factors?

2. Materials and methods

2.1. Study site

Tibet Autonomous Region (26°50'-36°53'N; 78°25'-99°06'E) is located in the south-western part of Tibetan Plateau. With average annual temperature of less than 5 °C and long sunshine duration of more than 3000 h per year, this region is well known for its harsh environment and fragile ecosystems. Frost occurs more than 6 months of the year and permafrost occurs over extensive parts of the region. The climate of the Tibetan Plateau is alternatively controlled by the Indian summer monsoon in the summer and westerlies in the winter. The total amount of annual precipitation varies from over 1,000 mm in the southeast to less than 50 mm in the northwest.

This region consists of Qiangtang Semi Arid Zone, South Tibetan Semi Arid Zone, Eastern Tibetan Semi Humid Zone and Eastern Himalayas South Slope Humid Area (Academician of Chinese Academy of Sciences 2001). The vegetation distribution follows the spatial distribution of humidity: Alpine Steppe grows in the western and northern part, Meadow Grassland grows in the middle and southern part, scrubs and mixed needle/broad leaved forest grows in the eastern part (Yang *et al* 2010, Zhang *et al* 2014) (Figure 1). The major vegetation type of this region is alpine grassland, served as the dominant food supply for animal husbandry of Tibetan communities. Alpine steppe consists of cold and xerophytic herbaceous plants such as *Stipa purpurea* and *Carex moorcroftii*, mixed with alpine forbs (e.g., *Polygonum viviparum*). Whereas, meadow grassland is dominated by perennial grasses such as *Kobresia pygmaea*, *K. humilis* and *K. tibetica*.

2.2. Data collection

2.2.1. NDVI data

The Normalized Difference Vegetation Index (NDVI), derived from the contrast between the red and near-infrared reflection of solar radiation, is commonly used to reflect the growth conditions of the vegetation activity. The latest version of the global vegetation inventory modelling and mapping studies (GIMMS) NDVI3g dataset was download from <https://nex.nasa.gov/nex/projects/1349/>. GIMMS NDVI3g datasets have been normalized to account for issues such as sensor calibration loss, orbital drift, and atmospheric effects such as volcanic eruptions (Pinzon and Tucker 2014). We followed He *et al* (2017) to do the cleaning (eliminating the Flag values from 3 to 7), then re-projected this NDVI3g data onto a geographic grid with WGS 1984 spheroid. We collected 32 years (1982–2013) of NDVI images with a temporal interval of 15 days and a spatial resolution of 1/12°.

2.2.2. Climate data

The Climatic Research Unit (CRU: University of East Anglia Climatic Research Unit, 2008) provides high resolution gridded datasets with global coverage. The data sets (CRU TS4.01, <https://crudata.uea.ac.uk/cru/data>) provide time

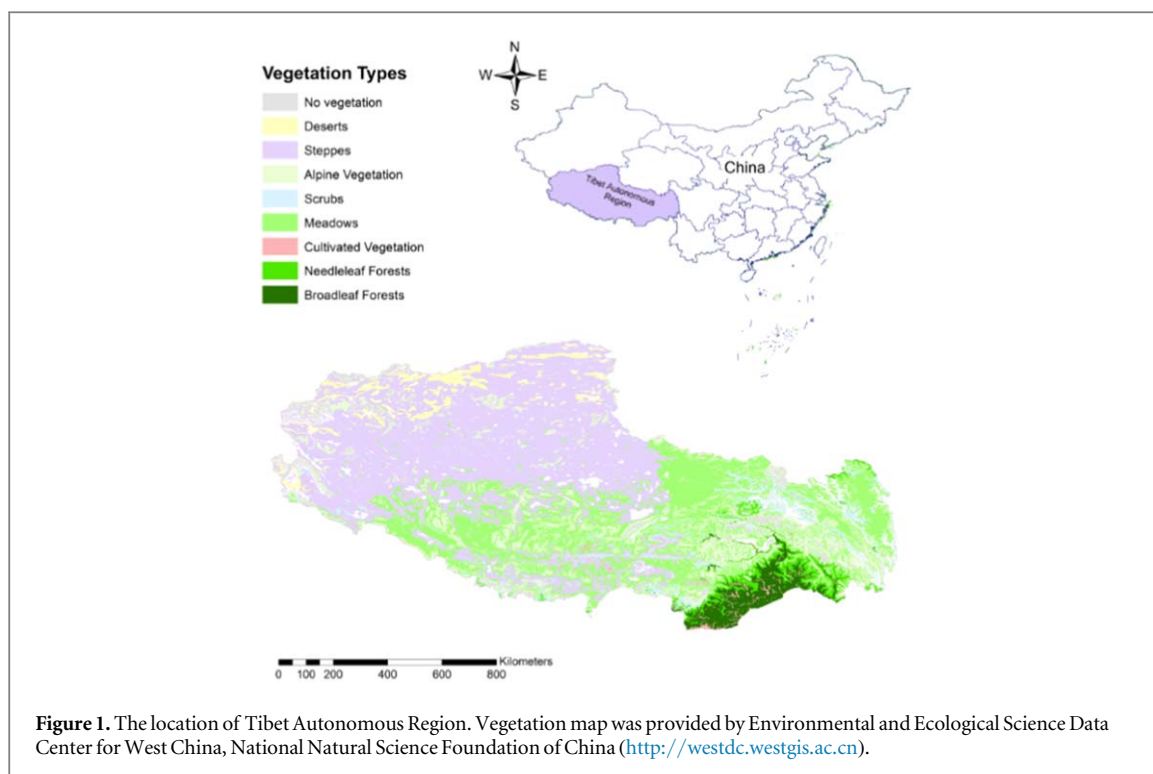


Table 1. Data Source and abbreviation of climate variables.

Abbreviation	Variables	Unit	Source/Method
CLD	Cloud cover	%	CRU TS v4.01
PRE	Precipitation	mm	CRU TS v4.01
TMP	Daily mean temperature	°C	CRU TS v4.01
TMN	Daily minimum temperature	°C	CRU TS v4.01
TMX	Daily maximum temperature	°C	CRU TS v4.01
VAP	Vapour pressure	hPa	CRU TS v4.01
PET	Potential evapotranspiration	mm	CRU TS v3.23
WMI	Warmth index of Kira, accumulate TMP above 5 °C	°C/month	(Kira, (1945))
CDI	Cold index of Kira, accumulate negative difference between TMP and 5 °C	°C/month	(Kira, (1945))
NDVI	Normalized Difference Vegetation Index	—	GIMMS ndvi3g

series for a range of climate parameters (Harris *et al* 2014). In the CRU processing scheme, several station-based data sources were harmonized to obtain most reliable estimates (table 1). After spatial interpolation and superposition on the reference climatologies, these anomalies constitute the final 0.5° grids global climate dataset (Mitchell and Jones 2005). We extracted the monthly data of climate variables from the year 1982 to 2013 and cropped the dataset by the regional boundaries. Then, the original CRU datasets were disaggregated using a bilinear interpolation function to match the GIMMS NDVI3g datasets spatially and temporally.

The threshold of 5 °C is considered as an important bio-climatic indicator in ecological studies especially for cold environment (Dong *et al* 2012). The continental vegetation distribution and species spatial distribution limits are supposed to be constrained by the accumulated temperature above/below this threshold (Kira 1991). In this study, Warm index (WMI) and cold index (CDI) (Kira 1945) were prepared for each pixel using equations (1) and (2), which counts the annual sum of positive and negative differences between monthly means and 5 °C. As the vegetation activity is mostly influenced by coldness before the growing season, the CDI in this study is counting the negative temperature difference (TMP-5 °C) between two consecutive summers.

$$WMI = \sum(TMP - 5) \quad (TMP \geq 5) \quad (1)$$

$$CDI = -\sum(5 - TMP) \quad (TMP < 5) \quad (2)$$

2.3. Methods

2.3.1. Trend analysis

We analyzed the trends of climatic variables and vegetation activities with the Mann–Kendall test (Mann 1945, Hamed 2008). As serial autocorrelation could influence the trend significance detected by Mann–Kendall test, a pre-whitening procedure (MK-TFPW) was conducted to reduce the influence of autocorrelation on the significance of Mann–Kendall test results (Yue and Wang 2002). Then, the Mann–Kendall test was applied to prewhitened temperature series. Positive tau values of Mann–Kendall test indicated an increasing trend, whereas negative tau represented a decreasing trend. To detect the change points in these time series, the Mann–Whitney–Pettitt test was conducted (Pettitt 1979).

The slope of each variable was computed by simple linear regression against the year. Since a linear regression trend fails to represent the slope when abnormal anomalies are included in the time series, then the true slope (change per unit time) can be estimated by using a simple nonparametric procedure developed by Sen (1968), which is robust against outliers and has the ability to reject anomalies without affecting the slope. The Sen slope estimator is the median of the slopes computed for n values observed at all pairwise time steps for a total of $n \times (n-1)/2$ slopes.

2.3.2. Correlation analysis

Correlation analyses were conducted to reveal the relationship between climatic variables and vegetation activities. In consideration of the colinearity among the climate variables, the partial correlation coefficient between the NDVI and each climatic factor was calculated, with the other climatic factor acting as control variable. The partial correlation of time series of x_i and x_j given x_k is:

$$r_{ij|k} = \frac{r_{ij} - r_{ik}r_{jk}}{\sqrt{1 - r_{ik}^2}\sqrt{1 - r_{jk}^2}} \quad (3)$$

Where $r_{ij|k}$ is the partial correlation coefficient between x_i and x_j controlling x_k , r_{ij} is the correlation coefficient between x_i and x_j , r_{ik} is the correlation coefficient between x_i and x_k , r_{jk} is the correlation coefficient between x_j and x_k .

2.3.3. Principal regression analysis

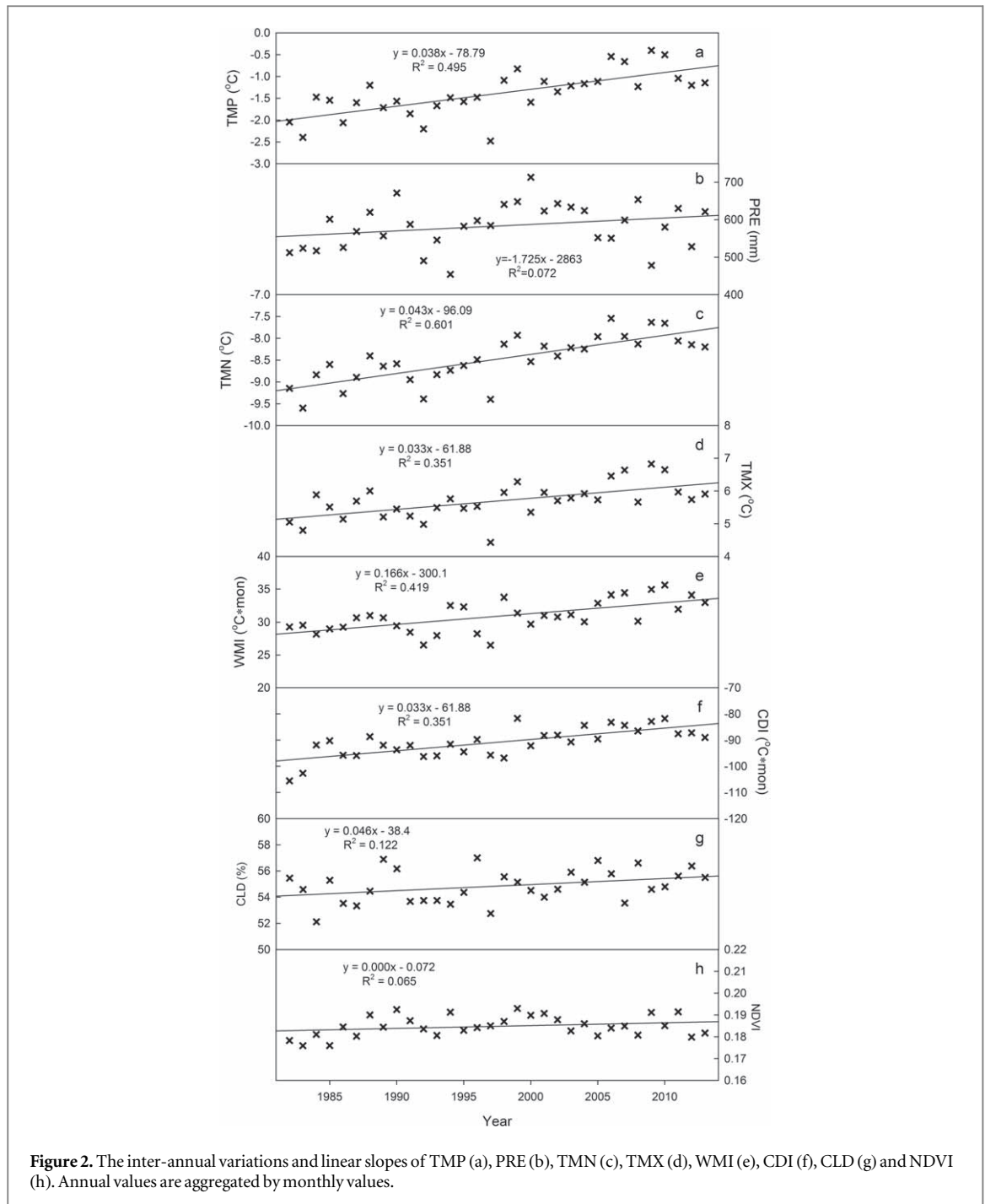
To reveal the spatial pattern of climate-vegetation interaction and eliminate the co-linearity among climate variables, we used principal components regression (PCR) to identify the vegetation sensitivities to the correlated climate variables. In each pixel, all time series of climate variables and NDVI were transformed to z-score anomalies using long-term mean and standard deviation. For the data frame of climate variables, principal component analysis was conducted to extract the major principals and the correlated climate variables. Then the loadings of each variables were multiplied by the coefficients derived from regression analysis between standardized NDVI and the major principals. Finally, the relative importance of each climate variables in driving the changes in NDVI can be revealed and then plotted. All of the calculations were conducted in R (R Core Team 2014).

3. Results

3.1. Climate change and trend analyses

Figure 2 and table 2 displayed the results of time series analysis for climate variables and vegetation activities. From 1982 to 2013, TMP had a positive trend of 0.38°C per decade. Higher trend in TMN (0.44°C per decade) than TMX (0.34°C per decade) implies the asymmetric warming and decreasing diurnal temperature range. The linear trend of CDI ($4.33^\circ\text{C}\cdot\text{month}\cdot 10\text{ yr}^{-1}$) is 2.6 times higher than WMI ($1.66^\circ\text{C}\cdot\text{month}\cdot 10\text{ yr}^{-1}$), indicating the widely reported pronounced winter warming. Despite annual precipitation (PRE) increased with a slope of 17.25 mm per decade, NDVI had an insignificant positive trend over the past decades, indicating the complicated interaction between vegetation growth and climate change.

A significant change point around the year 1997/1998 was detected in time series of temperature regime. From 1982 to 1997, TMP, TMN, TMX, WMI and CDI had slightly increased, whereas, their slopes had greatly increased since 1998 (table 2). By contrast, PRE had a moderate positive rate of $17.80\text{ mm}\cdot 10\text{ yr}^{-1}$ from 1982 to 1997, followed by great decreasing rate of $-47.94\text{ mm}\cdot 10\text{ yr}^{-1}$ from 1998 to 2013. The time series of CLD is characterized by significant positive trend but insignificant change point, which is different from the temporal patterns of PRE and temperature regime.



3.2. Correlation and principal component analyses

Table 3 shows that, NDVI had an insignificant Pearson correlation coefficient but a significant Kendall correlation coefficient with PRE, indicating the nonlinear relationship between PRE and NDVI. Significant Pearson correlations between temperature regime (TMP, TMX, CDI) and NDVI suggests the complicated controlling factors of NDVI inter annual variation.

Partial Pearson correlation analysis shows that the correlation coefficient ($R_{NDVI-TMP, PRE}$) between NDVI and TMP (controlling PRE) is higher than $R_{NDVI-PRE, TMP}$ (correlation coefficient between NDVI and PRE when TMP is controlled), suggesting the higher NDVI sensitivity to TMP (table 4). Whereas, Kendall and Spearman methods revealed a contrary result, indicating the complicated climate-vegetation relationship. Table 4 also revealed that NDVI has high sensitivities to TMX and CDI than TMN and WMI respectively, indicating the higher importance of TMX and CDI in driving NDVI inter annual variation.

Spatially, more pixels display the significant positive partial correlation between NDVI and TMP (21.62%, controlled PRE), compared with 7.35% of pixels that display the significant positive partial correlation between NDVI and PRE (controlled TMP). A proportion of 14.49% pixels displays positive partial correlation between

Table 2. Time series analyses of climatic variables and NDVI over the past 3 decades (1982–2013). All of the calculations were based on the annual values aggregated by the monthly values.

	TMP (°C)	TMX (°C)	TMN (°C)	WMI (°C·month)	CDI (°C·month)	PRE (mm)	PET (mm)	VAP (hPa)	CLD (%)	NDVI
MK-tau	0.52	0.44	0.58	0.46	0.50	0.21	0.23	0.42	0.26	0.16
pwmk-tau	0.26	0.28	0.21	0.23	0.23	0.15	0.17	0.23	0.29	0.06
Sen slope (per 10 yr)	0.18 ^a	0.23 ^a	0.12 ^a	0.98 ^a	1.63 ^a	16.09	3.81	0.05 ^a	0.61 ^b	0.00
Linear slope (per 10 yr)	0.38 ^a	0.34 ^a	0.44 ^a	1.66 ^a	4.33 ^a	17.25	5.45 ^b	0.10 ^a	0.47	0.00
Change point year	1997 ^a	1997 ^a	1997 ^a	1997 ^a	1998 ^a	1995	1997 ^b	1994 ^a	2002	1987
Slope (1982–1997)	0.04	−0.08	0.16	−0.28	3.81	17.80	−12.28 ^b	0.15	−0.01	0.00
Slope (1997–2013)	0.46 ^b	0.50	0.43 ^b	1.89	4.35 ^b	−47.94	11.59	0.06	0.89	−0.00

^a Correlation is significant at the 0.01 level (2-tailed).

^b Correlation is significant at the 0.05 level (2-tailed).

Table 3. Correlation analysis of climate variables and NDVI. All of the calculations were based on the annual values which were aggregated by monthly values.

Correlation analyses	Correlation coefficients		
	Pearson	Kendall	Spearman
TMP	0.356 ^a	0.233	0.356 ^a
TMN	0.340	0.202	0.312
TMX	0.351 ^a	0.266 ^a	0.382 ^a
WMI	0.193	0.153	0.216
CDI	0.419 ^a	0.238	0.352 ^a
PET	0.210	0.145	0.224
VAP	0.342	0.209	0.304
PRE	0.321	0.310 ^a	0.396 ^a
CLD	-0.086	-0.060	-0.117

^a Correlation is significant at the 0.05 level (2-tailed).

Table 4. Partial correlation analyses between NDVI and the comparable climatic variables.

Partial correlation	NDVI			Proportion of significant pixels	
	Pearson	Kendall	Spearman	Positive	Negative
$R_{NDVI-TMP, PRE}$	0.312	0.187	0.279	21.62%	7.17%
$R_{NDVI-PRE, TMP}$	0.271	0.278 ^a	0.332	7.35%	2.68%
$R_{NDVI-TMX, TMN}$	0.113	0.178	0.234	9.71%	3.78%
$R_{NDVI-TMN, TMX}$	0.066	0.024	-0.029	6.32%	7.62%
$R_{NDVI-WMI, CDI}$	-0.053	0.057	0.006	3.92%	3.78%
$R_{NDVI-CDI, WMI}$	0.382 ^a	0.193	0.284	14.49%	2.94%

^a Correlation is significant at the 0.05 level (2-tailed).

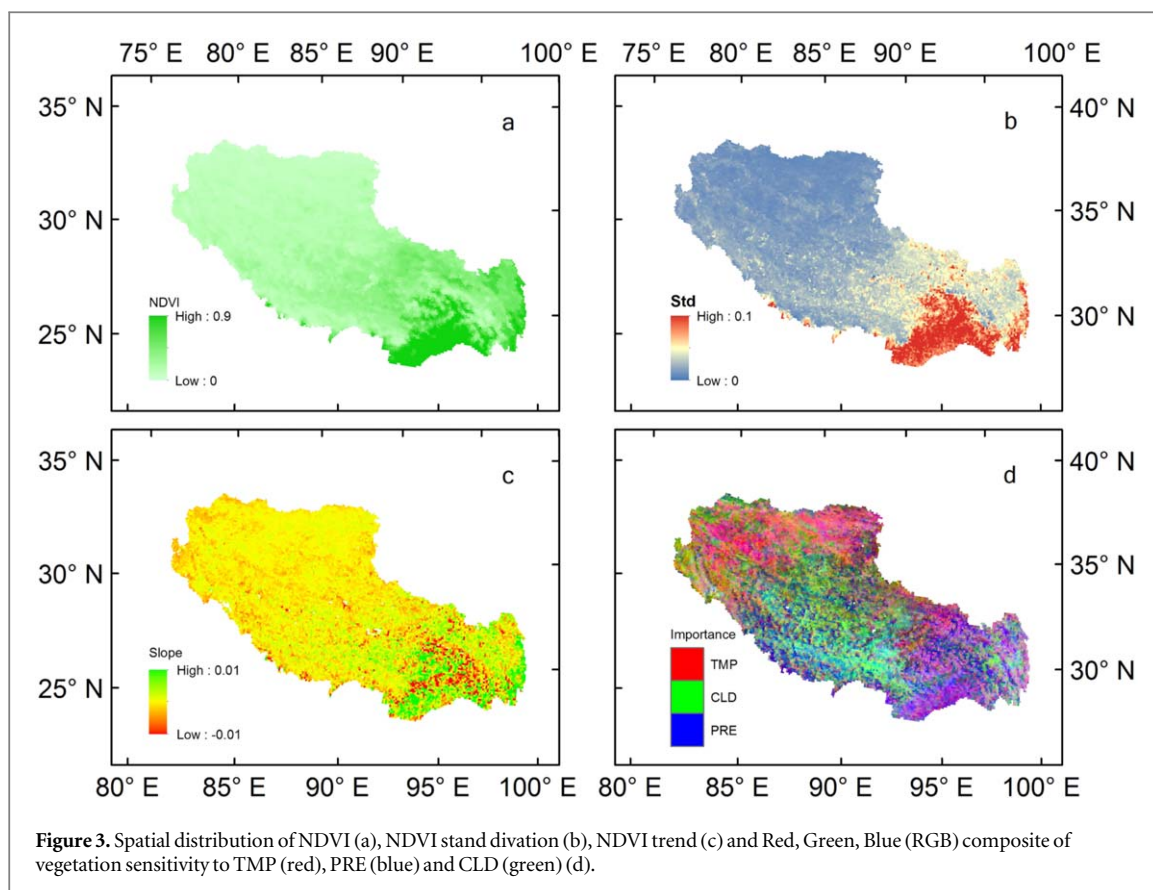
Table 5. Correlation coefficients and principal regression coefficients (PRC) between climate variables and the principal components.

Correlation matrix	PC1	PC2	PC3	PC4	PC5	PC6	PC7	PC8	PC9	PRC
TMP	0.992	0.048	-0.011	-0.017	-0.014	-0.107	0.033	-0.027	0.000	0.005
TMN	0.977	-0.137	0.054	-0.058	-0.031	-0.030	0.132	0.013	0.000	0.030
TMX	0.950	0.229	-0.075	0.024	0.003	-0.175	-0.066	-0.065	0.000	-0.021
WMI	0.848	0.144	0.297	0.286	0.201	0.220	-0.006	-0.034	0.000	0.002
CDI	0.855	0.016	-0.204	-0.352	-0.257	0.192	-0.034	-0.007	0.000	0.330
PET	0.685	0.666	-0.067	-0.160	0.223	-0.027	-0.027	0.083	0.000	-0.007
VAP	0.783	-0.408	-0.093	0.410	-0.194	-0.026	-0.040	0.064	0.000	0.129
PRE	0.246	-0.760	-0.525	-0.067	0.286	0.025	-0.007	-0.007	0.000	0.251
CLD	0.326	-0.667	0.610	-0.262	0.059	-0.049	-0.043	0.017	0.000	-0.289
Cumulative variance	0.615	0.807	0.896	0.949	0.980	0.995	0.998	1.000	1.000	—

NDVI and CDI (controlled WMI) whereas, only 3.92% of pixels displays positive partial correlation between NDVI and WMI (controlled CDI).

3.3. Principal regression analysis

Principal component analysis revealed that, the 1st principal component is highly correlated with TMP, TMN and TMX, representing the temperature component (table 5). The 2th principal component is highly correlated with PRE, representing the humidity component. And the 3th principal component is highly correlated with CLD, representing the radiation component. The first 6 principals explained more than 99.9% of variance. Using the principal regression coefficients as the importance, CDI has the highest importance in controlling NDVI, CLD and PRE ranks the second and the third importance respectively.



3.4. Spatial distribution of climate-vegetation relationship

Spatially, high values of NDVI and NDVI standard deviation are distributed in the eastern part covered by densely vegetation (figures 3(a), (b)). And pixels of significant positive NDVI trends are mostly located in eastern part (figure 3(c)). The negative NDVI trends are mostly located along the middle reaches of Yalu Tsangpo River.

Using TMP, PRE and CLD as the independent variables, principal regression analysis revealed that the alpine steppe of western part is mostly sensitive to temperature, the meadow grassland of middle part is mostly sensitive to humidity and the scrubs/mixed needle leaved and broad leaved forest in eastern part is relatively sensitive to radiation (figure 3(d)).

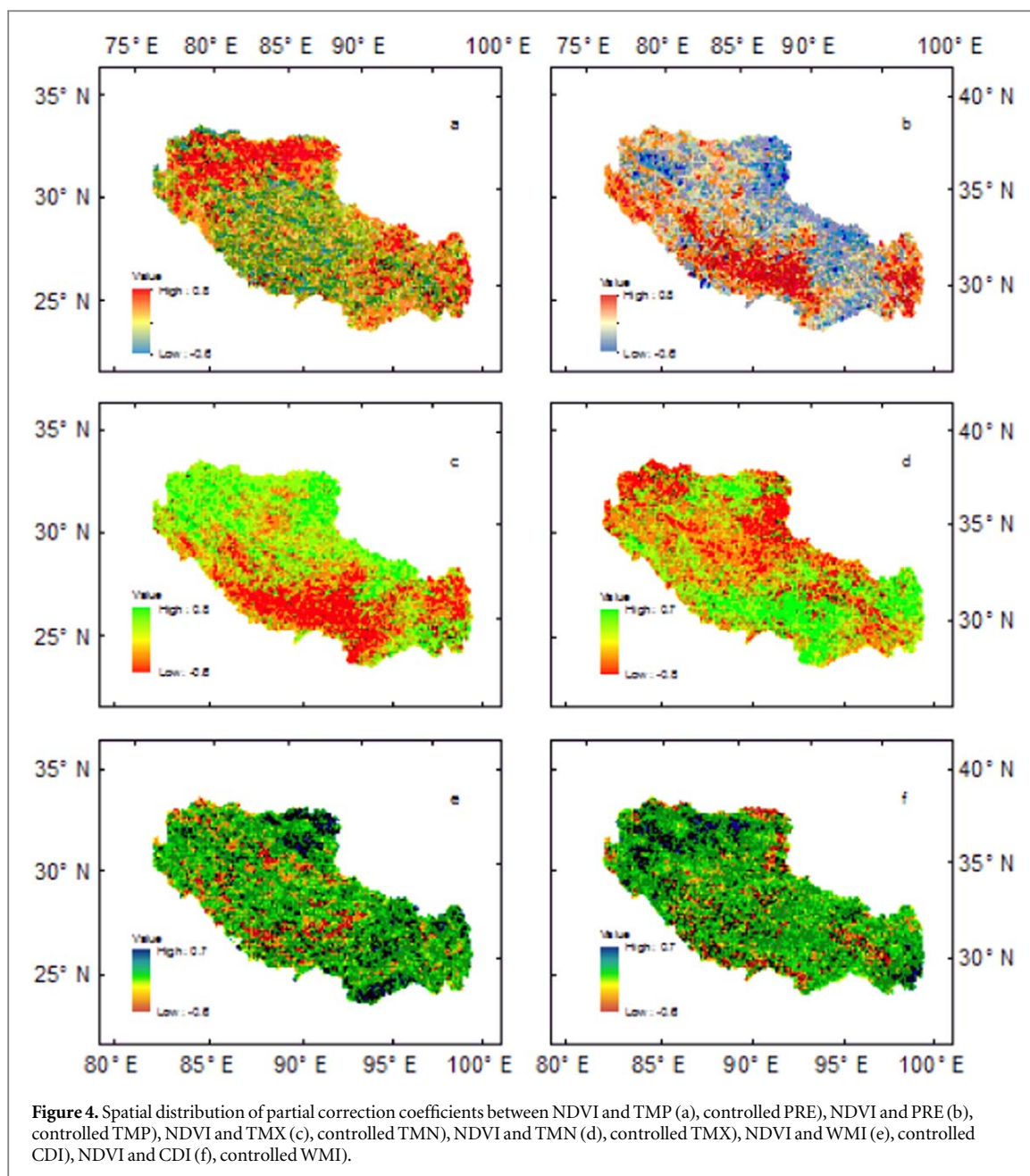
In order to reveal the spatial distribution of relative importance that controls the vegetation growth, partial correlation analysis at pixel scale was conducted. TMP has higher importance than PRE in northern Tibet Autonomous Region (figure 4(a)). Whereas, PRE has higher importance than TMP in South Tibetan Semi Arid zone (figure 4(b)). The impact of TMX is higher than TMN in most of the Tibet Autonomous Region, whereas, the impact of TMN is more important than TMX in Yalu Tsangpo River overlapped with the regions with high sensitivity to PRE. Region with high partial correlation between NDVI and WMI (controlled CDI) is located in northern part and forest distributed southeastern edge (figure 4(e)). Whereas, regions with high sensitivity to CDI (figure 4(f)) nearly overlaps with the regions with high sensitivity to TMP (figure 4(a)).

4. Discussion

4.1. Characteristics of climate change and vegetation growth

In this study, air temperature showed a strong trend of 0.38 °C per decade, which was higher than the global average level (Pachauri *et al* 2014). Combined with the positive trend in PRE, the regional climate change can be characterized as warming and wetting (Kuang and Jiao 2016). The greater warming trends in CDI and TMN than WMI and TMX represent the widely reported asymmetric warming (Liu and Chen 2000, Xia *et al* 2014). As diurnal minimum temperature is considered to be influenced by the surface long wave radiation (You *et al* 2017), the increased cloud coverage is accountable for the increased TMN and the decreased diurnal temperature range (You *et al* 2016).

The significant change point around the year 1998 is coincided with the climatic change point in Mediterranean (Jemai *et al* 2017), North Korea (Nam *et al* 2016), southwest China (You *et al* 2013) and the world famous 1997/1998 El Niño year (Bhaskaran and Mullan 2003, Cai *et al* 2014). The negative trend of



precipitation in post-1998 period coincided with the weakened Indian summer monsoon (Kulkarni 2012, Marotzke and Forster 2015).

As a result of regional climate change especially for the change of thermal growing season length (Dong *et al* 2012), NDVI has a positive trend over the past decades, which is in line with the previous reports of regional vegetation greening (You *et al* 2016) and surface albedo decreasing (Tian *et al* 2014). Spatially, the positive trends of NDVI are mostly distributed in eastern part of the region, which is coincided with the previous studies of regional phenology changes (Ding *et al* 2013) and vegetation growth (Zhang *et al* 2014).

This study also reveals the scattered pixels with negative NDVI trend (mostly distributed along the Yalunzangbu river), implying the ecological effects of land cover change, grassland degradation, urbanization, deforestation and desertification (Cui and Graf 2009, Shen *et al* 2012). Therefore, the ecological service might have reduced in eastern region (Tang *et al* 2018), despite the regional climate warming and wetting over the past decades.

4.2. Driving factors for vegetation activity

The asymmetric warming and its impact on vegetation activity has been reported by Zu *et al* (2018). The limited impacts of TMX and WMI on NDVI variation suggests the insignificant role of warmth in controlling the vegetation growth, which is contradicted with the warmth-limited regions such as boreal biomes (Peng *et al* 2013). The high

importance of TMN on controlling vegetation growth revealed in this study complies with the previous report of correlation between TMN and vegetation greenness over the Tibetan Plateau (Shen *et al* 2016).

The insignificant regional NDVI trend and complicated driving factors can be attributed to the spatial distribution of vegetation types (Zhong *et al* 2010). As the Tibet Autonomous Region consists of the alpine steppe in the northern and western part, the meadow grass in the middle and eastern part, and the shrub/mixed needle leaved and broad leaved forest in the eastern part, principal regression analysis revealed the 3 different patterns of controlling factors corresponding to the spatial distribution of the 3 vegetation types. Previous studies had also reported the different ecological consequences of climate change determined by different vegetation types (Sun *et al* 2016, Zhang *et al* 2018).

In this region, observed PRE is only a fraction of moisture availability for vegetation growth. The glacier melting, degradation of permafrost were neglected in this study. Previous study showed that, winter warming and greater TMN slope were considered as the indicators of permafrost degradation and water variability (Liu *et al* 2011). As a result, region with significant partial correlation between NDVI and TMN (controlled TMX) overlaps with the mass loss in southeastern Tibet and along the Himalayas (Song *et al* 2013, Pritchard 2019).

5. Conclusion

This study reveals the regional climate warming and wetting. The significant change point around the year of 1997/1998 coincides with the occurrence of global El Niño event and the starting of weakening India Monsoon. The regional NDVI had an insignificant positive trend with an insignificant change point, indicating the complicated climate-vegetation relationship. The asymmetric warming and the high importance of CDI and TMN possibly reflect the ecological effects of glacier melting and permafrost degradation.

Spatial distribution of controlling factors represents the spatial distribution of vegetation types. Alpine steppe is sensitive to temperature, meadow grassland is sensitive to humidity, and mixed needle leaved and broad leaved forest in eastern part is relatively influenced by radiation. The scattered negative NDVI trend implies the ecological effects of land cover changes, grassland degradation, urbanization, deforestation and desertification resulting from the increased human activity. Further studies are needed to reveal the impact of the asymmetric warming on the regional carbon/water flux and carbon/water balance.

Acknowledgments

This research was supported by National Key Research and Development Plan of China (2017YFC0506605) and Ecological Red Line Protection and Management Program, Ministry of Ecology and Environment, China. We thank National Aeronautics and Space Administration (NASA), CRU (Climate Research Union), Environmental and Ecological Science Data Center for West China, National Natural Science Foundation of China (Cold and Arid Regions Science Data Center at Lanzhou) for providing the free data access. R software team is appreciated for time-saving calculation. We thank the anonymous reviewers for valuable suggestions and comments on the manuscript.

Declaration of interest

None

Additional information

The authors declare that they have no competing interests.

ORCID iDs

Guangyong You  <https://orcid.org/0000-0002-3204-7597>

References

- Academicians of Chinese Academy of Sciences 2001 *1:1000,000 Vegetation Atlas of China* (Beijing: Science Press (in Chinese))
- Bhaskaran B and Mullan A 2003 El Niño-related variations in the southern Pacific atmospheric circulation: model versus observations *Clim. Dyn.* **20** 229–39
- Cai W *et al* 2014 Increasing frequency of extreme El Niño events due to greenhouse warming *Nat. Clim. Chang.* **4** 111

- Cong N, Shen M, Yang W, Yang Z, Zhang G and Piao S 2017 Varying responses of vegetation activity to climate changes on the Tibetan Plateau grassland *Int. J. Biometeorol.* **61** 1433–44
- Cui X and Graf H-F 2009 Recent land cover changes on the Tibetan Plateau: a review *Clim. Change* **94** 47–61
- Ding M, Zhang Y, Sun X, Liu L, Wang Z and Bai W 2013 Spatiotemporal variation in alpine grassland phenology in the Qinghai-Tibetan Plateau from 1999 to 2009 *Chinese Sci. Bull.* **58** 396–405
- Dong M, Jiang Y, Zheng C and Zhang D 2012 Trends in the thermal growing season throughout the Tibetan Plateau during 1960–2009 *Agric. For. Meteorol.* **166–167** 201–6
- Guo B, Zhou Y, Wang S and Tao H 2014 The relationship between normalized difference vegetation index (NDVI) and climate factors in the semiarid region: a case study in Yalu Tsangpo River basin of Qinghai-Tibet Plateau *J. Mt. Sci.* **11** 926–40
- Hamed K H 2008 Trend detection in hydrologic data: the Mann—Kendall trend test under the scaling hypothesis *J. Hydrol.* **349** 350–63
- Harris I, Jones P D, Osborn T J and Lister D H 2014 Updated high-resolution grids of monthly climatic observations—the CRU TS3.10 Dataset *Int. J. Climatol.* **34** 623–42
- He Y, Lee E and Warner T A 2017 A time series of annual land use and land cover maps of China from 1982 to 2013 generated using AVHRR GIMMS NDVI3g data *Remote Sens. Environ.* **199** 201–17
- Huang K *et al* 2016 The influences of climate change and human activities on vegetation dynamics in the Qinghai-Tibet Plateau *Remote Sens.* **8** 876
- Jemai S, Ellouze M and Abida H 2017 Variability of precipitation in arid climates using the wavelet approach: case study of watershed of Gabes in South-East Tunisia *Atmosphere (Basel)* **8** 178
- Kim Y, Kimball JS, Zhang K and McDonald K C 2012 Satellite detection of increasing Northern Hemisphere non-frozen seasons from 1979 to 2008: implications for regional vegetation growth *Remote Sens. Environ.* **121** 472–87
- Kira T 1991 Forest ecosystems of east and southeast Asia in a global perspective *Ecol. Res.* **6** 185–200
- Kira T 1945 *A New Classification of Climate in Eastern Asia as the Basis for Agricultural Geography* (Kyoto, Japan Horticulture: Inst. Kyoto Univ.)
- Kuang X and Jiao J J 2016 Review on climate change on the Tibetan Plateau during the last half century *J. Geophys. Res. Atmos.* **121** 3979–4007
- Kulkarni A 2012 Weakening of Indian summer monsoon rainfall in warming environment *Theor. Appl. Climatol.* **109** 447–59
- Kumar K R, Pant G B, Parthasarathy B and Sontakke N A 1992 Spatial and subseasonal patterns of the long-term trends of Indian summer monsoon rainfall *Int. J. Climatol.* **12** 257–68
- Liu J, Xie J, Gong T, Wang H and Xie Y 2011 Impacts of winter warming and permafrost degradation on water variability, upper Lhasa River, Tibet *Quat. Int.* **244** 178–84
- Liu X and Chen B 2000 Climatic warming in the Tibetan Plateau during recent decades *Int. J. Climatol.* **20** 1729–42
- Mann H B 1945 Nonparametric tests against trend *Econom. J. Econom. Soc.* **13** 245–59
- Marotzke J and Forster P M 2015 Forcing, feedback and internal variability in global temperature trends *Nature* **517** 565–70
- Mitchell T D and Jones P D 2005 An improved method of constructing a database of monthly climate observations and associated high-resolution grids *Int. J. Climatol.* **25** 693–712
- Nam W-H, Hong E-M and Baigorria G A 2016 How climate change has affected the spatio-temporal patterns of precipitation and temperature at various time scales in North Korea *Int. J. Climatol.* **36** 722–34
- Pachauri R K *et al* 2014 Climate change 2014: synthesis report *Contribution of Working Groups I, II and III to the Fifth Assessment Report of the Intergovernmental Panel on Climate Change (IPCC)* (<https://doi.org/10.1017/cbo9781107415416.008>)
- Peng S *et al* 2013 Asymmetric effects of daytime and night-time warming on Northern Hemisphere vegetation *Nature* **501** 88–92
- Pettitt A N 1979 A non-parametric approach to the change-point problem *Appl. Stat.* **28** 126–135
- Pinzon J and Tucker C 2014 A non-stationary 1981–2012 AVHRR NDVI3g Time Series *Remote Sens.* **6** 6929–60
- Pritchard H D 2019 Asia's shrinking glaciers protect large populations from drought stress *Nature* **569** 649–54
- R Core Team 2016 R: A language and environment for statistical computing. R Foundation for Statistical Computing, Vienna (<https://www.R-project.org/>)
- Sen P K 1968 Estimates of the regression coefficient based on Kendall's tau *J. Am. Stat. Assoc.* **63** 1379–89
- Shen M, Piao S, Chen X, An S, Fu Y H, Wang S, Cong N and Janssens I A 2016 Strong impacts of daily minimum temperature on the green-up date and summer greenness of the Tibetan Plateau *Glob. Chang. Biol.* **22** 3057–66
- Shen M, Piao S, Cong N, Zhang G and Janssens I A 2015 Precipitation impacts on vegetation spring phenology on the Tibetan Plateau *Glob. Chang. Biol.* **21** 3647–56
- Shen W, Li H, Sun M and Jiang J 2012 Dynamics of aeolian sandy land in the Yarlung Zangbo River basin of Tibet, China from 1975 to 2008 *Glob. Planet. Change* **86–87** 37–44
- Shi C *et al* 2019 Growth response of alpine treeline forests to a warmer and drier climate on the southeastern Tibetan Plateau *Agric. For. Meteorol.* **264** 73–9
- Song C, Huang B and Ke L 2013 Modeling and analysis of lake water storage changes on the Tibetan Plateau using multi-mission satellite data *Remote Sens. Environ.* **135** 25–35
- Sun J, Qin X and Yang J 2016 The response of vegetation dynamics of the different alpine grassland types to temperature and precipitation on the Tibetan Plateau *Environ. Monit. Assess.* **188** 20
- Tang Z, Sun G, Zhang N, He J, Wu N, Tang Z, Sun G, Zhang N, He J and Wu N 2018 Impacts of land-use and climate change on ecosystem service in eastern Tibetan Plateau, China *Sustainability* **10** 467
- Tian L, Zhang Y and Zhu J 2014 Decreased surface albedo driven by denser vegetation on the Tibetan Plateau *Environ. Res. Lett.* **9** 104001
- Wang C, Guo H, Zhang L, Liu S, Qiu Y and Sun Z 2015 Assessing phenological change and climatic control of alpine grasslands in the Tibetan Plateau with MODIS time series *Int. J. Biometeorol.* **59** 11–23
- Xia J *et al* 2014 Satellite-based analysis of evapotranspiration and WATER balance in the Grassland ecosystems of DRYLAND East Asia *PLoS One* **9** e97295
- Yang Y, Fang J, Fay P A, Bell J E and Ji C 2010 Rain use efficiency across a precipitation gradient on the Tibetan Plateau *Geophys. Res. Lett.* **37** 1–5
- Yang Z, Shen M, Jia S, Guo L, Yang W, Wang C, Chen X and Chen J 2017 Asymmetric Responses of the End of Growing Season to Daily Maximum and Minimum Temperatures on the Tibetan Plateau *J. Geophys. Res. Atmos.* **122**
- You G, Zhang Y, Schaefer D, Sha L, Liu Y, Gong H, Tan Z, Lu Z, Wu C and Xie Y 2013 Observed air/soil temperature trends in open land and understory of a subtropical mountain forest, SW China *Int. J. Climatol.* **33** 1308–16
- You Q, Jiang Z, Wang D, Pepin N and Kang S 2017 Simulation of temperature extremes in the Tibetan Plateau from CMIP5 models and comparison with gridded observations *Clim. Dyn.* **51** 355–69

- You Q, Min J, Jiao Y, Sillanpää M and Kang S 2016 Observed trend of diurnal temperature range in the Tibetan Plateau in recent decades *Int. J. Climatol.* **36** 2633–43
- Yue S and Wang C Y 2002 Applicability of prewhitening to eliminate the influence of serial correlation on the Mann-Kendall test *Water Resour. Res.* **38** 4-1-4-7
- Zeppel M J B, Wilks J V and Lewis J D 2014 Impacts of extreme precipitation and seasonal changes in precipitation on plants *Biogeosciences* **11** 3083–93
- Zhang L, Guo H, Wang C, Ji L, Li J, Wang K and Dai L 2014 The long-term trends (1982–2006) in vegetation greenness of the alpine ecosystem in the Qinghai-Tibetan Plateau *Environ. Earth Sci.* **72** 1827–41
- Zhang Q, Kong D, Shi P, Singh V P and Sun P 2018 Vegetation phenology on the Qinghai-Tibetan Plateau and its response to climate change (1982–2013) *Agric. For. Meteorol.* **248** 408–17
- Zhong L, Ma Y, Salama M S and Su Z 2010 Assessment of vegetation dynamics and their response to variations in precipitation and temperature in the Tibetan Plateau *Clim. Change* **103** 519–35
- Zhu W, Jiang N, Chen G, Zhang D, Zheng Z and Fan D 2017 Divergent shifts and responses of plant autumn phenology to climate change on the Qinghai-Tibetan Plateau *Agric. For. Meteorol.* **239** 166–75
- Zu J, Zhang Y, Huang K, Liu Y, Chen N and Cong N 2018 Biological and climate factors co-regulated spatial-temporal dynamics of vegetation autumn phenology on the Tibetan Plateau *Int. J. Appl. Earth Obs. Geoinf.* **69** 198–205